A new surface accumulation map for western Dronning Maud Land, Antarctica, from interpolation of point measurements

Gerit ROTSCHKY,[1] Per HOLMLUND,[2] Elisabeth ISAKSSON[3], Robert MULVANEY,[4]
Hans OERTER,[1] Michiel R. VAN DEN BROEKE,[5] Jan-Gunnar WINTHER[3]

[1]*Alfred Wegener Institute for Polar and Marine Research, P.O. Box: 120161, 27515 Bremerhaven, Germany*
E-mail: grotschky@awi-bremerhaven.de
[2]*Department of Physical Geography, Stockholm University, S-106 91 Stockholm, Sweden*
[3]*Norwegian Polar Institute, Polar Environmental Centre, N-9296 Tromsø, Norway*
[4]*British Antarctic Survey, Natural Environment Research Council, Madingley Road, Cambridge CB3 0ET, England*
[5]*Institute for Marine and Atmospheric Research Utrecht, P.O. Box 80.005, Utrecht University, Princetonplein 5,
3584 CC Utrecht, The Netherlands*

ABSTRACT

As a result of intensive field activities carried out by several nations over the last 15 years a set of accumulation measurements for western Dronning Maud Land (DML), Antarctica, was collected, based on firn-core drilling and snow-pit sampling. This new information was supplemented by earlier data taken from the literature, resulting in 111 accumulation values. Using Geographical Information Systems software, a first region-wide mean annual snow-accumulation field was derived. In order to define suitable interpolation criteria, the accumulation records were analysed with respect to their spatial autocorrelation and statistical properties. The resulting accumulation pattern resembles well known characteristics such as a relatively wet coastal area with a sharp transition to the dry interior, but also reveals complex topographic effects. This work furthermore identifies new high-return shallow drilling sites by uncovering areas of insufficient sampling density.

INTRODUCTION

Over the last decades much effort has been put into recovering possible changes in the mass budget and dynamics of polar ice sheets in response to climate-change. Mass-balance estimates require knowledge of the amount and spatial distribution of snow accumulation, which still suffers from large uncertainties. Shallow firn and ice cores, supplemented by snow pits, are traditionally used to derive the accumulation and climate history throughout the last centuries. As a result from precipitation variations and wind-driven redistribution of snow, surface accumulation rate is spatially as well as temporally highly variable. Local values depend on the overall climate, regional weather conditions and terrain characteristics at macro to micro scale. For example, Reijmer and Van den Broeke (2003) found standard deviations in 4-7 years accumulation averages to range from 20% to 70% of the average annual accumulation, based on data of several automatic weather stations in Dronning Maud Land (DML). On an annual scale, large horizontal accumulation variations have been observed from stake measurements by Melvold and others (1998) reaching up to 500 kg m^{-2} a^{-1} over a distance of less then 3 km on Jutulstraumen. In this respect ice cores serve as a useful tool because they provide long-term averaged accumulation rates which more likely represent a typical value for their surrounding area. However, due to the time-consuming and often costly procedure of firn-core drilling, their numbers remain limited.

Sampling density of accumulation records varies strongly over the Antarctic ice sheet (Vaughan and others, 1999). Drilling sites are usually concentrated along traverse routes and easily accessible coastal regions. The sparse and uneven data distribution sets high demands on interpolation techniques used to map the broad scale accumulation distribution over wider regions. Furthermore it is questionable, whether firn-core records covering different accumulation periods can be combined in a single map if trends in accumulation history cannot be precluded. Nevertheless, for most regions, firn cores still represent the only in-situ source of information that can be used for accumulation compilations.

DML has been under investigation by several countries over the last 50 years resulting in a large body of available literature. This region is particularly interesting because of its sensitivity to conditions over the Atlantic sector of the Southern Ocean, possibly connecting it with the climate record of the Greenland ice sheet. Field activities increased in the 1990's in the framework of the International Trans-Antarctic Scientific Expedition (ITASE), established in order to gain a greater understanding of Southern Hemisphere climate within the last 200 years, and due to pre-site surveys for the European Project for Ice Coring in Antarctica (EPICA), aiming at locating a suitable deep ice-core drilling site in the Atlantic sector of East Antarctica.

As more and more data on accumulation rates have successively been compiled each season, it becomes necessary to summarize and combine the information for a region wide picture and estimation of snow accumulation in DML. So far no accumulation map

exists specifically for western DML that is based entirely on in-situ data. In this paper, we present a complete set of reliable accumulation records available at the time of this study for the western DML region. For a spatial interpolation we apply algorithms based on geostatistical methods and exploratory data analysis. By doing so we aim at recovering the large-scale accumulation pattern, resulting from overall climate, weather, and topographic conditions. Clearly, small scale accumulation variations cannot be resolved using point data. Prior to this our dataset is discussed in terms of its spatial and temporal validity. By this we justify the combination of unevenly distributed field data representing a variety of accumulation periods at each location.

GEOGRAPHICAL DESCRIPTION OF WESTERN DML

Morphology

The area of investigation is stretching inland from the Antarctic coast at 70°S to about 80°S, enclosed by the 20°W and 15°E meridians (Fig.1). Based on its topography, western DML can be subdivided into four regions: (1) the major ice shelves Riiser-Larsenisen, Ekströmisen, and Fimbulisen, (2) the lower inland ice regions Ritscherflya and Hellehallet, and (3) the high-altitude plateau area with an elevation above 2500 m a.s.l., i.e. the Wegener Inlandeis made up by Amundsenisen and Wegenerisen. A clear borderline between coastal / lower inland ice regions and the plateau consists of (4) the nunatak areas of the Heimefrontfjella, Kirwanveggen, and Mühlig-Hofmann-Gebirge mountain ranges, which penetrate the ice-sheet reaching heights of about 2700 m a.s.l.. Acting as a barrier to air masses approaching from the Weddell Sea and the Atlantic Ocean to the north this chain of mountains has large impact on the accumulation distribution, separating the area into two distinct accumulation regimes.

The surface topography of the plateau is smooth with wind-shaped features, i.e. small-size sastrugi (10-15 cm high) (Stenberg and others, 1998) indicating that the mean wind velocities in this part of Antarctica are moderate. Undulations with amplitudes on the metre-scale and wavelengths on the kilometre-scale have been linked to bedrock morphology (e.g. Budd and Carter, 1971; Rotschky and others, 2004). Large areas of Amundsenisen have been delineated as ice drainage basin feeding the Filchner Ice Shelf with the ice divide as far north as 75°S (Giovinetto and Bentley, 1985). Major outlets from Amundsenisen are Stancomb-Wills Ice Stream, draining into the Brunt Ice Shelf, and Jutulstraumen, feeding Fimbulisen. With an area of approximately 124 000 km², Jutulstraumen is the largest ice stream within our area of investigation. Topography varies much stronger coastward of the nunataks, where drainage basins alternate with mountain ridges. Varying slope gradients and aspects as well as a variable surface-wind field introduce complex patterns in the accumulation distribution (Van den Broeke and others, 1999).

General characteristics of snow accumulation

DML is situated in the Atlantic sector of Antarctica, and in the sphere of influence of cyclonic systems that move along the coast, the strongest winds blow from the east
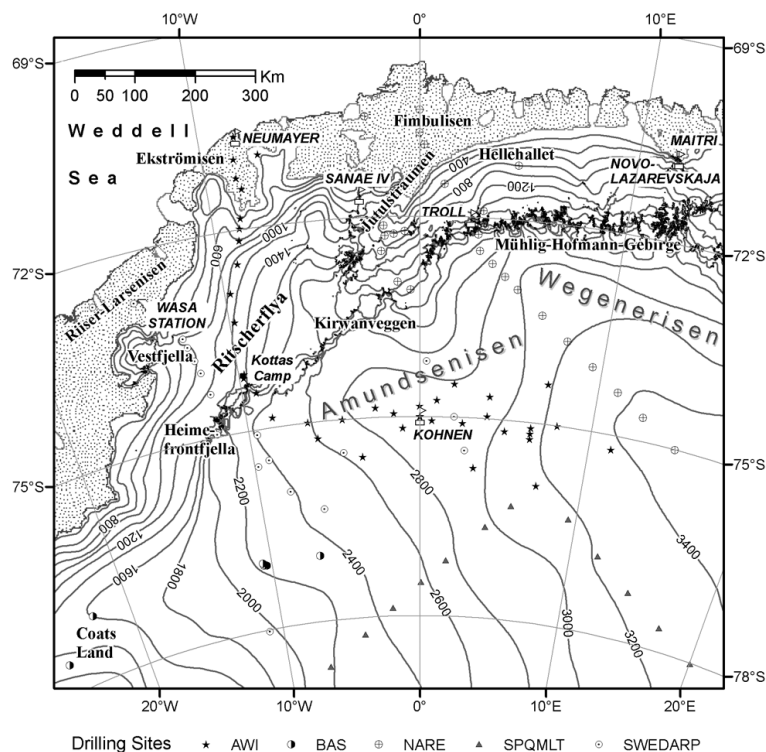

Figure 1. Area of investigation and sampling network. Varying symbols for point records were chosen in order to distinguish between different institutions involved in data acquisition. Elevation contours in 200 m intervals are given as solid black lines.

to northeast (Lunde, 1961). Field observations reveal a typical continental precipitation distribution with a general decrease in accumulation with increasing elevation and distance from the open ocean, and with decreasing mean annual air temperature, respectively (Giovinetto and others, 1990; Vaughan and others, 1999). In DML, the nunataks interrupt this steady modification by forcing the humid air masses to rise, resulting in accumulation extremes of up to 780 kg m^{-2} a^{-1} on Jutulstraumen, as reported by Melvold and others (1998) based on stakes measurements for a 1 year period. Large regional variations in accumulation occur in dependence of predominant cyclone pathways, topographic disturbances, and katabatic wind activity (Richardson and Holmlund, 1999; Van den Broeke and others, 1999; King and others, 2004). A detailed discussion of precipitation and related snow accumulation characteristics in DML was presented by Noone and others (1999).

SAMPLING FRAMEWORK

Our dataset includes accumulation data from snow pit studies as well as from firn and ice core drillings carried out by six nations during 20 different Antarctic field campaigns, held over a time period of about four decades. Compiled records are listed in the Appendix with a reference, tabulated by site name, campaign name and year of observation. Because of the susceptibility to errors we did not consider records based on snow pit stratigraphy alone. Results of this method have been criticised as being generally unreliable due to the subjective interpretation. Total obliteration of the annual layering resulting from strong metamorphism or wind erosion is held responsible for usual overestimations of accumulation rates derived from firn stratigraphy, particularly where accumulation is low (e.g. Picciotto and others, 1971; Giovinetto and Zwally, 2000; Frezzotti and others, 2004).

Sporadic visits to DML already began with the Norwegian-British-Swedish Antarctic Expedition in the years 1949-52, however, systematic data acquisition on accumulation did not start before the late 1960's. The earliest reliable dataset originates from the third leg of the U.S. South Pole-Queen Maud Land traverse (SPQMLT 1964-68) covering the southernmost part of the area of interest between 75°S to 80°S and between 10°W to 40°E on Amundsenisen (Picciotto and others, 1971). Here the dating of 17 snow pits was based on total β-activity deposited after nuclear weapon tests. Data acquisition continued with German activities resulting in a number of 9 firn cores drilled within two seasons (1981/82 and 1986/87) at locations near the Georg-von-Neumayer station on the Ekström Ice Shelf (Schlosser and others, 1999) and on Ritscherflya (Oerter and others, 1999). Glaciological work conducted in the frame of the Swedish Antarctic Research Program (SWEDARP) in the seasons 1988/89 (Isaksson and Karlén, 1994) and 1991/1992 (Isaksson and others, 1996; this paper) included a number of 11 shallow firn cores along a traverse route starting at the Riiser-Larsenisen Ice Shelf across Ritscherflya towards Amundsenisen east of the Heimefrontfjella mountains.

The latter area was visited again during the Swedish ITASE campaigns in 1993/1994, providing accumulation data based on snow pits dated by multi-parameter chemical records (Stenberg and others, 1998). Collaborative Swedish/Norwegian/Dutch activities continued in 1997/98 within EPICA including snow pit studies (Stenberg and others, 1999) as well as medium depth ice-core drillings at Camp Victoria (Karlöf and others, 2000) and a depot of the British Antarctic Survey (BAS) (Hofstede and others, 2004). Within five consecutive seasons from 1995/96 until 99/2000 EPICA traverse work under the leadership of the German Alfred Wegener Institute (AWI) retrieved more than 30 shallow firn and 3 medium depth ice cores with the majority taken on Amundsenisen, but also close to Neumayer station, in the Heimefrontfjella, and on Ritscherflya (Oerter and others, 1999 and 2000; this paper).

Within an extensive mass balance and glacier research project the Fimbulisen and Jutulstraumen region was traversed by several Norwegian Antarctic Research Expeditions (NARE) in the seasons 1992/93 (Melvold and others, 1998; Melvold, 1999) and 1993/94. They recovered a number of 12 shallow firn cores. In 1996/97 a Norwegian/Swedish/Dutch ground traverse as part of EPICA drilled 15 firn-cores along a traverse from Fimbulisen passing Hellehallet and Mühlig-Hofmann-Gebirge and on the plateau along the ice divide leading to the Japanese deep drilling site at Valkyrjedomen (called Dome F). Those records define the eastern boundary of our investigation area (Isaksson and others, 1999; Van den Broeke and others, 1999). NARE field workers in collaboration with Dutch scientists also recovered two medium depth ice cores on Amundsenisen in 2000/01 (Hofstede and others, 2004) and on Fimbulisen (Kaczmarska and others, 2004). BAS expeditions retrieved 2 shallow firn cores in the season 1986/87 (Wolff and Suttie, 1994) and 1987/88 (Mulvaney and Wolff, 1993), the only records available in Coats Land, the south-western corner of the investigated area. Ten years later, in 1997/98, BAS in joint venture with NARE participated in EPICA studies with 3 shallow firn cores (this paper) and one medium depth ice core on Amundsenisen (Hofstede and others, 2004). The latest available record at the time of writing results from AWI firn core drilling near Heimefrontfjella in 2003/04 (this paper).

SPATIAL AND TEMPORAL VALIDITY OF DATA

Annual local noise and small-scale spatial variability

Spatial and temporal variations in accumulation are attributed to the combined effects of (1) airmass transport pathways, (2) interaction of airflow with topography, and (3) local effects, i.e. sastrugi and redistribution by snowdrift. Post-depositional processes driven by wind reshape the primary precipitation pattern leading to preferential accumulation of material in topographic depressions, in contradiction to the lowered accumulation rates that we find on crests (e.g. Sommer and others, 2000; Arnold and Rees, 2003; Frezzotti and others, 2005). Complex local wind erosion and re-deposition processes occur due to undulations in surface topography at the kilometre scale and more specifically

on variations of the downslope surface gradient (e.g. Melvold and others, 1998). King and others (2004) observed large spatial variability in snow accumulation (20–30% on a scale of around 1 km) even for gentle topography, which was attributed to a highly nonlinear relationship between wind speed and snow transport. Stake line readings and ice-penetrating radar (IPR) studies provide continuous accumulation information at high spatial resolution (Richardson-Näslund and others, 1997; Richardson-Näslund 2004; Spikes and others, 2004; Rotschky and others, 2004). For instance Isaksson and Karlén (1994) found a standard deviation of 70% of the average annual accumulation using stake measurements at Ritscherflya. Such results raised questions on how representative single point records are at a regional scale. Their spatial scale of significance has been widely discussed and is a critical point when interpolating over large distances.

Locally highly variable snow deposition patterns are preserved in the form of a considerable inter-annual variability generally detected in firn core stratigraphy. This phenomenon has been discussed in a large body of literature (e.g. Goodwin, 1991; Frezzotti and others 2004 and 2005). Specifications for year-to-year variations range from 30% on Amundsenisen (Sommer and others, 2000) to as high as 250% for firn cores drilled on Jutulstraumen (Melvold and others, 1998). High-frequency variability in annual layer thickness within ice cores are agreed to be associated in the first place with wind redistribution controlled by micro-relief, rather than to climatically forced precipitation changes (Frezzotti and others, 2005; Reijmer and Van den Broeke, 2003). As a consequence, accumulation time series generally miss a clear correspondence even for nearby firn core sites (Sommer and others, 2000). Such findings indicate that only multi-year accumulation averages should be used for regional studies. A number of 5-10 years is generally considered sufficient for providing reliable estimates of local snow accumulation (Petit and others, 1982; Mosley-Thompson and others, l985; Morgan, 1985). We account for this fact by excluding all records that cover less than 5 years of accumulation in order to avoid biases in our interpolation map resulting from annual local noise and small-scale spatial variability. When having a choice between several measurements taken at the same location, we decided for the one with the longer average time interval.

Multi-decadal accumulation trends

Both positive and negative long-term trends of snow accumulation have been reported over the Antarctic Ice Sheet, e.g. Petit and others (1982), Morgan and Goodwin (1991), Mosley-Thompson (1992). Our dataset consists of records that are irregularly sampled in space and time, covering a wide variety of accumulation time periods. Average time intervals range from several years to several hundreds of years with the majority (78 out of 111) less than 50 years. Sampling was carried out over a time period of roughly 40 years (see Appendix). Therefore, differences in accumulation values might partly originate from a changing accumulation rate over time. Consequently, those could induce misinterpretations when modelling spatial variations statistically in order to define optimal interpolation criteria for applying geostatistical surface prediction methods, i.e. kriging (see section Surface Prediction below). It must therefore first be investigated, whether this dataset is suitable for compiling an accumulation map.

All investigators involved in data sampling agree that time series of accumulation rates and stable isotopes do not indicate a drastic change in atmospheric moisture transport in DML over the covered time periods of their studies (e.g. Karlöf and others, 2000; Melvold, 1999; Isaksson and others, 1996; Oerter and others, 1999). At decadal time scales, the records show no clear trend or different magnitude and direction in changes between the single sites. Oerter and others (1999) and Graf and others (2002) observed temporal variations for the last two centuries in central DML that were linked to temperature variations derived from stable isotopes records. However, for the same region constant accumulation rates characterized the last 2,000 years in three intermediate depth ice cores (Sommer and others, 2000). Slight increases or decreases in accumulation rates over several decades were found to be small compared to interannual variability. This is in accordance with findings of Isaksson and others (1996) and Hofstede and others (2004) who combined information from different sites on Amundsenisen. We found a stable plateau climate by comparing cores M with M150 (see Appendix). Both were drilled at 75°00'S/15°00'E and cover a time period of 31 years and 1033 years, respectively. Despite the different average-time intervals similar accumulation values of 43 and 45 kg m^{-2} a^{-1}, respectively, indicate stable accumulation rates for the longest time interval included in this study.

Coastal areas experience stronger climatic fluctuations since they are exposed to the combined effects of changing sea ice extent and cyclonic activity (Isaksson and Karlén, 1994; Kaczmarska and others, 2004). However, since observed changes (e.g. Isaksson and others, 1996; Melvold, 1999) are generally restricted in time, show alternating signs and no inter-site correlation, a likely explanation is the movement of a bore-hole site through a complex undulation pattern related to bedrock topography (Melvold and others, 1998; Sommer and others, 2000). Depending on ice-flow velocity and wavelength of surface undulations, which is of the order of some kilometres (Richardson-Näslund and others, 1997; Rotschky and others, 2004; Eisen and others, 2005), a coring site requires several decades to travel from a low accumulation surface crest to a high accumulation surface hollow. For this reason an apparent trend may be detected from changes in annual-layer thickness of firn cores, even in stable climatic periods. However, the average accumulation derived from the affected firn core would still be representative for a larger surrounding area. Based on these data, we assume that no major change in accumulation occurred in western DML during the past 1000 years that would significantly corrupt the quality of a spatially interpolated picture of accumulation rates over our area of interest.

EXPLORATORY SPATIAL DATA ANALYSIS

Nearly all 111 selected accumulation records result from traverse work conducted by different nations as described above. Therefore, data collection did not follow an optimal sampling procedure. The resulting sampling density varies and remains relatively small considering the well-known high spatial variability of snow accumulation, particularly in mountainous areas. In order to define suitable parameters for a spatial interpolation we first examined the statistical properties of our dataset, i.e. value distribution, spatial variability, and global spatial trends.

Value distribution

Accumulation records range from as low as 19 kg m^{-2} a^{-1} at the south-eastern corner of our study area on Amundenisen to a maximum of 491 kg m^{-2} a^{-1} on Jutulstraumen. By looking at the number of records measured within defined accumulation intervals in steps of 20 kg m^{-2} a^{-1}, we find our dataset not to be normally distributed (Fig. 2). A bell-shaped histogram would be required for an optimal interpolation result. Instead, the majority of records are lower than 200 kg m^{-2} a^{-1}, causing the histogram bars to be clearly shifted to the left. The highest number of records (36) fall into the accumulation interval between 45 and 65 kg m^{-2} a^{-1}, while medium and higher values are obviously underrepresented in our dataset. This skewness is also expressed by a large difference between the median (63.5 kg m^{-2} a^{-1}) and the mean value (129.49 kg m^{-2} a^{-1}), which in turn is of the same order as the standard deviation of 124.67 kg m^{-2} a^{-1}. The considerably higher proportion of low data values within the dataset is clearly due to the preferential sampling on the DML plateau area (75 out of 111 records). Data points with values higher than 200 kg m^{-2} a^{-1} are without exception located near the coast and the adjacent lower inland regions north of the nunataks, while nearly all records below this threshold belong to the inland plateau. Already from this frequency distribution two separate accumulation regimes can be distinguished.
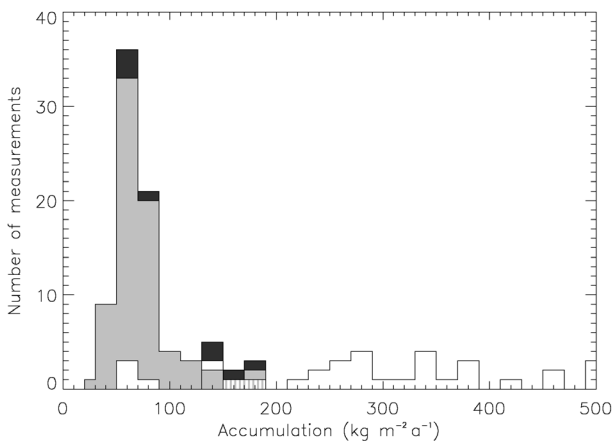

Figure 2. Frequency distribution of accumulation rates. In grey: records sampled on the plateau (generally below 200 kg m^{-2} a^{-1}), white: coastal records, and in black: total number.

Table 1. Statistics of accumulation-value distribution in kg m^{-2} a^{-1}.

	Total	Coast	Plateau	Plateau Log. Transf.
No. records	111	36	75	75
Mean	130	271	62	4.04
Median	64	271	56	4.03
Min	19	46	19	2.94
Max	491	491	171	5.14
Std. dev.	124.2	128.2	30.0	0.42
Skewness	1.46	-0.06	1.86	0.37

By looking at the accumulation values separately for coastal and plateau regions, we find a distribution close to normal for the coast, expressed by similar mean and median values (Table 1). The coastal records account for the high standard deviation in our dataset, with a value of 128.2 compared to only 30.0 kg m^{-2} a^{-1} for the plateau. The latter is in agreement with findings of Oerter and others (1999). The higher spread in accumulation values for the coastal data is not surprising, considering the complex geographical nature described earlier. However, the relative standard deviation is similar for both regions. For the subset of records located on the plateau a distribution close to normal can be achieved by performing a logarithmic transformation of our data values. By this we can adjust the coefficient of skewness, a measure of the symmetry of a distribution, which should be near zero for optimal interpolation results.

For individual regions within the area of investigation we find distinct differences in accumulation mean and spread (Fig. 3). We are aware that the number of records is a critical factor for such comparisons, particularly for the nunatak areas. Amundsenisen and Wegenerisen exhibit their smooth topography and remote location with low spread and values generally lower than 120 kg m^{-2} a^{-1}. In contrast, the data are highly variable for coastal regions. The most striking region is Jutulstraumen, which covers the entire range of accumulation values within our dataset. This large spatial variation in accumulation has been attributed to strong erosion and re-deposition processes on the ice stream controlled by surface undulations and a complex near surface wind field (Holmlund and Näslund, 1994). Accumulation extremes also result from increased precipitation between 900 and 1200 m elevation due to orographic uplift and adiabatic cooling of humid air masses (Melvold and others, 1998).

Outliers

Outliers within a dataset can dramatically affect the performance of a surface prediction by distorting the variogram modelling associated with the kriging procedure later used for the interpolation. They should therefore be identified prior to the interpolation (Burrough, 1986). Within our dataset no global outliers exist, i.e. no records are very high or low relative to all
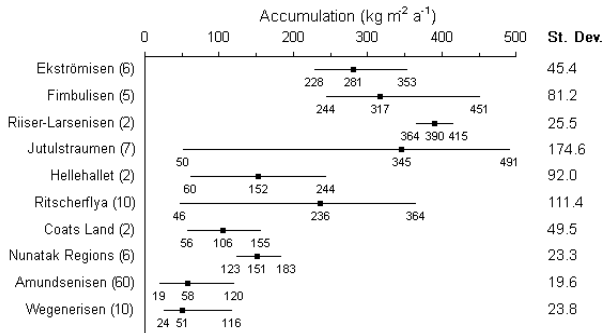
Figure 3. Minima, mean, and maxima of accumulation rates for individual regions. The number of respective records is given in brackets.

of the values. However, on four locations we find sample points within the normal range of the entire dataset, but exhibiting unusually low values relative to their surrounding neighbours. Major accumulation deficits are found for core sites Jut_E (72°13'S, 00°43'W) and Jut_I (71°31'S, 01°11'W), both located on Jutulstraumen, which have been linked to strong katabatic wind activity as indicated by wind crusts, sastrugi and nearby blue ice fields (Melvold and others, 1998). Anomalous low values also characterize core sites B10_11 (72°30'S, 09°06'W) and "km 270" (72°56'S, 09°41'W), situated on Ritscherflya at an elevation of around 1000 m a.s.l.. From field observations and isotope analysis it was found that these low values are also due to erosion by wind activity, not caused by lower precipitation rates (Oerter and others, 1999). From stake line readings (Rotschky and others, 2006) and IPR measurements (Richardson-Näslund and others, 1997) we know that those core sites are situated within a wider zone of very low accumulation rates, which is likely a consequence of strong katabatic winds originating in the Heimefrontfjella range. We can therefore conclude that all those local outliers have been measured correctly and represent real abnormalities, reflecting the high spatial accumulation variability in complex terrain. We expect that measuring errors are not a major problem for an interpolation of the dataset.

Global spatial trends

To identify global spatial trends we examined possible relationships between snow accumulation and distance to the nearest coast, elevation as well as slope gradient and orientation. Those variables are often used to explain the general distribution of snow accumulation rates (e.g. Giovinetto and others, 1990; Bernhard and Weibel, 1999). Terrain information was extracted from the RAMP digital elevation model (Liu and others, 2001). The ice front was taken from the Antarctic Digital Database (ADD) version 4, provided by the Scientific Committee on Antarctic Research (SCAR). Using the entire dataset, we did not find a correlation between accumulation rates and the chosen parameters. For instance, both the lowest (46 kg m^{-2} a^{-1}) and highest (491 kg m^{-2} a^{-1}) coastal values are found within the elevation interval of 900 to 1100 m a.s.l. at a distance of 200 to 250 km from the coast. Even on the flat ice shelves,

Table 2. Global trends. Correlation coefficients (R) between accumulation rates and elevation as well as distance to the coast.

Distance Interval (km)	No. records	R	Elevation Interval (m a.s.l.)	No. records	R
150 - 1000	75	-0.60	1300 - 3500	75	-0.60
400 - 1000	58	-0.61	2000 - 3500	72	-0.57
500 - 1000	37	-0.68	2500 - 3500	55	-0.52
600 - 1000	17	-0.80	3000 - 3500	26	-0.51

accumulation ranges from 228 to 451 kg m^{-2} a^{-1}. Clear cross-correlations between slope gradient and accumulation reported by Melvold and others (1998) or King and others (2004) apply only for limited areas.

Excluding all coastal records from the analysis yields an expected negative cross-correlation between accumulation and elevation as well as distance to the nearest coast each with R = -0.6. As in Giovinetto and others (1990) we can describe those relations using first and second order regression functions (Fig. 4). Concerning continentality, the correlation improves when moving gradually away from the coast (Table 2). The best correlation of R = -0.8 we find for the distance interval of 700 to 1000 km from the coast, indicating that other reasons for spatial accumulation variations (e.g. surface undulations) become less important inland.
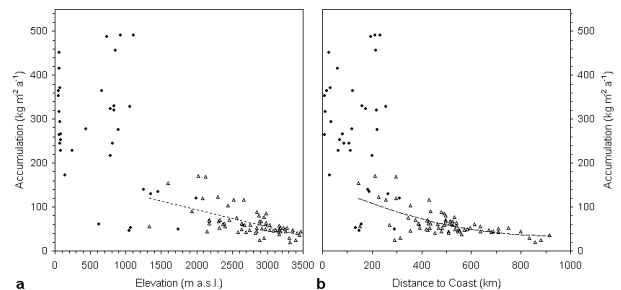
Figure 4. Global trends. Correlations between accumulation rates and (a) elevation as well as (b) distance to the coast. Coastal records are given as black dots, triangles indicate records sampled on plateau regions.

SURFACE PREDICTION

Semi-variogram modelling

The process of variogram modelling, i.e. variography, is an instrument for characterizing the spatial variability of a dataset. It gives useful information for selecting optimal interpolation parameters, e.g. the mathematical model to be used for computing efficient interpolation weights, the size and shape of the search window, as well as the number of neighbouring measurement sites to be included in the prediction of unsampled sites. In order to estimate accumulation rates for the western DML region we use kriging as geostatistical interpolation

method. Fundamental to kriging is the assumption that a relationship exists between the location of sites and the measured values, which can be modelled statistically. In theory the difference of values should be the same between any two points that are the same distance and direction apart. Naturally, dissimilarities between records increase with distance since nearby samples tend to be more alike than those farther apart. The degree of spatial autocorrelation is estimated from the data based on a scatter plot of half of the squared difference between pairs of sample values against their spatial separation h, called the semi-variogram cloud. An average of dissimilarities $y*(h)$ is calculated for all sample pairs falling into a certain distance bin of defined size, i.e. the lag size. The theory concerning kriging is discussed in more detail by Burrough (1986) and Wackernagel (1998).

Interpolation settings

Following the exploratory spatial data analysis, the dataset was separated into coastal and inland sites in order to define a set of domain-specific interpolation criteria. Different statistical properties suggest to use two local rather than a single global model for an interpolation, even though for the coastal domain the number of records becomes a critical factor for achieving a stable semi-variogram. The Heimefrontfjella, Kirwanveggen, and Mühlig-Hofmann-Gebirge mark the borderline between both data subsets. To improve the western boundary conditions, where data are missing over large distances we used data from Coats Land for both domains.

The selection of a proper set of interpolation parameters is highly subjective. However, we found that the resulting patterns remained quite stable for reasonable values of tested interpolation parameters. Even the specific variogram model type, used for computing interpolation weights, seems to be of minor influence. Over the smooth plateau region, where accumulation variability is relatively small, we selected a spherical model type which shows a progressive decrease of spatial autocorrelation until some distance, beyond which the autocorrelation becomes zero. For the coastal domain, a circular model type with a steeper curve near the origin, giving more weight to the closest neighbours for each prediction, is more appropriate. Variations in lag size and number did not significantly affect the output surface. A lag size of 20 km was chosen for both domains in order to get representative averages for semi-variogram bins.

Concerning the number of measured values to be used in a prediction, stable results are computed including at least 2 to 5 neighbours in all four directions. Any further increase in the number of neighbours has no impact on the resulting pattern because of the decreasing influence of remote points. The specific shape of the neighbourhood determines where to look for data points. A clear indication for selecting optimal search radii is given by the range of the semi-variogram cloud defining the distance to which data are statistically correlated (Burrough, 1986). Higher autocorrelation in one direction than in another might result from global trends

Table 3. Interpolation settings.

Settings	Coastal domain	Plateau domain (Interior region)
Geostatistical method	Ordinary kriging	Universal kriging
Transformation	none	Log
Trend	none	linear
Model type	spherical	circular
Lag Size (m)	20,000	
Lag No.	15	
Neighbours	5 at least 2 per search quarter	
Search window		
Anisotropy	No	Yes (NW -SE)
Axis angle	45°	65°
Major axis (km)	80 - 125	205 - 250
Minor axis (km)	80 - 125	105 - 150

and/or anisotropy. Our earlier spatial data analysis showed a first order trend on the plateau running from northwest to southeast towards increasing elevation and distance to coast, which was removed prior to variogram modelling and added back before predictions were made. From variography we still find anisotropic autocorrelation for this region, i.e. values in northeast-southwest direction change more slowly than perpendicular to this. Since such a phenomenon can be explained from topography and resultant predominant wind direction as modelled e.g. by Van Lipzig and others (2004), we assume that these directional differences are not a measurement artefact resulting from the preferential alignment of records along traverse lines which could lead to insufficient sampling density for robust estimates in all directions. Consequently we accounted for this anisotropic spatial autocorrelation by applying varying search radii as described in the following.

In general we found a single plateau record to be representative for a larger area than coastal records. This is in agreement with other findings (Stenberg and others, 1999). The spatial autocorrelations suggests that the search radii should be between 200 and 250 km from northeast to southwest and 100 to 150 km perpendicular to this direction. For the coastal domain, where major variation occurs over shorter distances, the search radius was kept as small as possible (between 80 to 125 km in any direction). Little variations in search radii led to evident changes in the predicted surface, particularly in the coastal area. Since the most efficient search radius remains subject of speculation, a good solution is to produce an average composite of 10 realisations, each time adjusting the search window by slightly enlarging its two axes (i.e. the search radii) in 5 km steps. The differences between these predictions are used as a measure of uncertainty in the predicted surface.

Having computed the experimental variograms and fitted model parameters, our accumulation records were interpolated using ordinary kriging for the coast and universal kriging for the plateau domain. The latter

should be applied only if an apparent spatial trend in the data can be explained from a priori knowledge (Burrough, 1986). Using a logarithmic transformation makes the data more normally distributed in case of the plateau domain. Here, the interpolation was carried out using the logarithmically transformed data which were then transformed back. In Table 3 our interpolation settings are summarized.

RESULTS AND DISCUSSION

Surface Prediction

The resulting accumulation distribution is mapped in Figure 5. Clearly, predicting a surface from sparse point data gives only a smoothed picture of the underlying reality. Details of spatial accumulation variability cannot be reproduced and the resulting pattern is highly dependent on the random distribution of sample points. For the coastal area, high accumulation alternates with accumulation lows reflecting a spatial variability in precipitation and snow transport that is topographically forced. Isolated circular patterns around single records result from values that deviate significantly from their surrounding neighbours. On the plateau, a clear trend of decreasing accumulation with increasing distance to coast and elevation from northwest to southeast (as described above) is reproduced. Values range from 150 kg m^{-2} a^{-1} just south of the mountain ridges down to as little as 25 kg m^{-2} a^{-1} near the south-eastern corner of our study area. Tongue-shaped patterns of higher

accumulation advance from coastal regions further inland, where nunatak barriers are absent over larger distances, for instance south of Jutulstraumen and Coats Land. Some problems are visible near Mühlig-Hofmann-Gebirge where predicted values at the northern margin of the plateau domain increase rapidly over short distances. In this area computed accumulation rates are unreliable. Interpolation difficulties occur furthermore where in situ data are missing over large distances between traverse lines running inland from the coast. The resulting striped patterns are clearly an artefact of the interpolator and not representative for the true accumulation.

Due to interpolation uncertainties in consequence of the sparse and uneven data sampling scheme, estimating the total surface mass balance in western DML is difficult. In spite of the larger area, the total accumulation on the plateau (58 · 10^4 km²) sums up to only 38 Gt a^{-1} versus 62 Gt a^{-1} for the coastal region with a spatial extent of 24 · 10^4 km². Discrepancies in total accumulation between our 10 slightly varied realisations are marginal (generally less than 1%). In Table 4 we compare our results with previous accumulation compilations by Vaughan and others (1999) and by Arthern and others (2006), who both guided the interpolation using background fields of satellite microwave observations, as well as by Huybrechts and others (2000), who applied a spline interpolation to nearly the same input data as in the present study. While the results of Vaughan and others (1999) and Huybrechts and others (2000) are 18% and 16% larger, respectively,
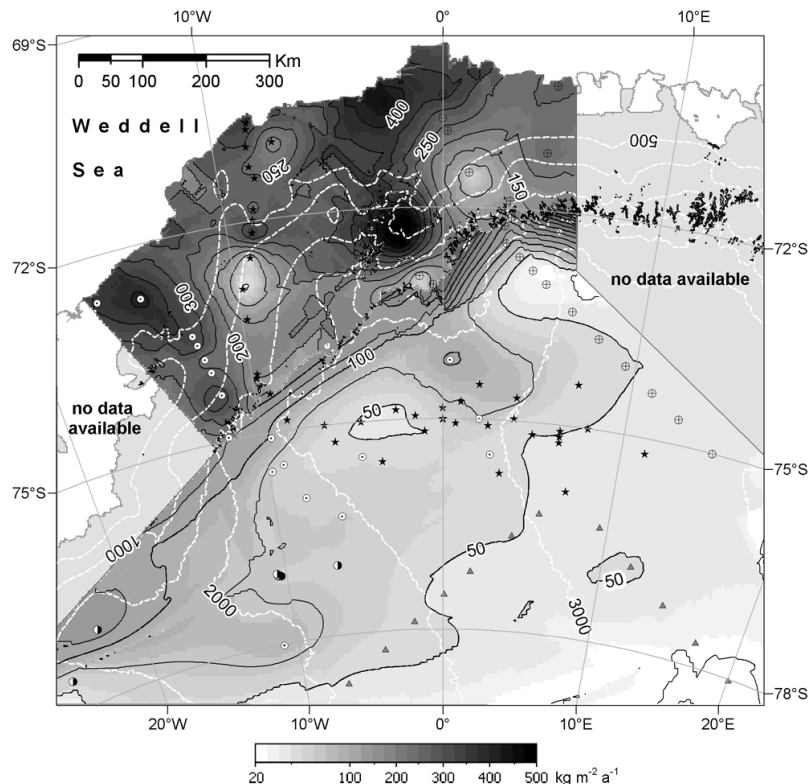
Figure 5. Contoured accumulation pattern for western DML (data available from the PANGEA Web site http://doi.pangaea.de/10.1594/PANGAEA.472297). A grey scale as well as contours at 50 kg m^{-2} a^{-1} (coastal domain) and 25 kg m^{-2} a^{-1} (plateau domain) are used to indicate the broad spatial variability in snow accumulation across the predicted area. Elevation contours in 500 m intervals are given as dashed white lines. The borderline between coastal and plateau domain follows the mountain chains and is shown as solid grey line.

the recently published findings by Arthern and others (2006) yield about 13% less accumulation for the western DML area than this study. These differences result from significantly higher estimates for the plateau in case of Vaughan and others (1999) and for the coastal area in case of Huybrechts and others (2000). In opposite, Arthern and others (2006) yield similar estimates for the plateau, their coastal estimates however are significantly lower than ours. Mainly the same input data have been used in all of the studies, which suggests that differences occur due to interpolation approaches. In general, spline interpolation may produce local artefacts of excessively high or low values if input values change dramatically over short distances. Therefore, the results of Huybrechts and others (2000) are unreliable for the DML coastal area. The main reason for disagreements we see in the absence of a barrier between the coastal and plateau accumulation regimes in earlier studies, which results in an overestimation of the area of validity of high accumulation coastal records in case of Vaughan and others (1999) and of low accumulation plateau records in case of Arthern and others (2006), respectively. Like those of Arthern and others (2006) our results indicate that snow accumulation in western DML is very probably smaller than previously assumed.

Interpolation accuracy

In general, accuracies vary across the predicted area with data sampling density. To evaluate the uncertainty of the interpolated surface, an error estimate is required. In absence of an extra set of independent observations randomly distributed across the predicted area, we
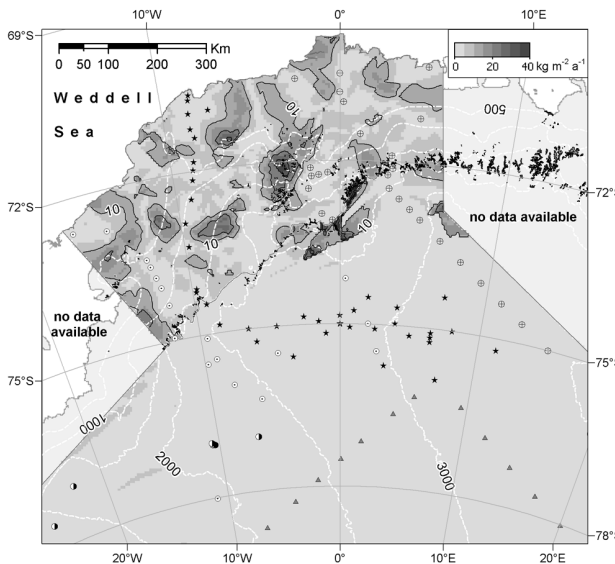
Table 4. Total accumulation in Western DML in Gt a^{-1}. Comparison between this study and earlier published results.

	Coastal domain	Plateau domain	Total	Difference %
this paper	62.0	37.7	99.7	-
Vaughan and others, 1999	63.4	54.5	117.9	+18.3
Huybrechts and others, 2000	74.5	41.3	115.8	+16.2
Arthern and others, 2006	49.1	37.4	86.5	-13.3

cannot quantify the accuracy directly. From the relatively small number of available data, a subset for validation purposes could not be created prior to interpolation. Each point in the dataset is essential for the variogram modelling and original prediction.

Some measure of certainty is provided as a by-product of the kriging procedure, known as the kriging variance. In the literature, this quantity has been criticised specifically as being ineffective and found to be a poor substitute for a true error (e.g. Journel, 1986; Chainey and Stuart, 1998). Basically, the kriging variance, depending only on the geometrical arrangement of the sample data points, simply states that accuracy decreases with growing distance from input data.

As a measure of confidence we instead used the differences between the 10 interpolation realisations, each with slight adjustments in the applied search window as described above. The lower the standard deviation of the different predictions, the more accurate the interpolation is likely to be in terms of self-consistency of the model applied to the data. The standard deviations across the predicted area are mapped in Figure 6, expressing a clear difference between coastal and plateau domains. On the plateau, data density seems sufficient for achieving stable interpolation results, with the exception of the Jutulstraumen inlet area. In contrast, for coastal regions, exhibiting a much larger spatial accumulation variation, major interpolation uncertainties occur for unsampled locations between measurement sites. Clearly, small adjustments in the shape of the search window impact mostly were single values deviate greatly from their surrounding neighbours (local singularities as described above). This result is leading back to the question, how representative single point records are for their wider surrounding. In order to catch the full range of accumulation variability occurring due to the complex coastal terrain and wind field conditions, further data acquisition should be carried out also in other directions than from north to south. Regional climate modelling may also help in this respect (Van den Broeke and others, 2006).

Figure 6. Map of standard deviation between 10 predictions with stepwise increase of search radii. The data are available from the PANGEA Web site http://doi.pangaea.de/10.1594/PANGAEA.472298. A grey scale and contours at 10 kg m^{-2} a^{-1} (black lines) indicate the interpolation inaccuracy. Elevation contours in 500 m intervals are given as dashed white lines. The borderline between coastal and plateau domain follows the mountain chains and is shown as solid grey line.

SUMMARY AND CONCLUSIONS

A set of 111 accumulation measurements from western DML is compiled and presented. Most data result from field work carried out over the last 15 years in the frame of EPICA and ITASE. Older records from literature are used to supplement the data. In spite of a large variety of covered accumulation periods, ranging between 5 and 1000 years, we find the datasets temporally representative as no significant trend in accumulation history over the last centuries has been reported from ice core records of this region. Uneven data distribution resulting from preferential alignment of measurement sites along traverse lines, which lead mostly inland from the coast, is a more critical factor for judging the spatial accumulation variability. Nevertheless, an interpolated map of mean annual snow accumulation rate could be derived that is in accordance with presumptions made from known overall spatial trends and topographically forced changes in accumulation. The interpolation was carried out using the geostatistical interpolation method of kriging, based on two local models and domain specific interpolation settings for coastal and inland sites. Our results suggest that the total accumulation rate for the predicted area is about 16% to 18% smaller than published in earlier years. For a quantitative evaluation of the uncertainty in predicted accumulation rates we calculated the standard deviation of 10 interpolation realisations each with slight stepwise increase in search radii. A map of the standard deviation thus obtained could help in locating future sampling sites to further minimize interpolation uncertainties. The existing sampling network should be improved with respect to surface topography and associated surface wind field patterns which in combination have the potential to change accumulation conditions dramatically over short distances, especially in the complex terrain of the coastal regions. These results are of interest for the interpretation of climate records from the study area as well as for ongoing surface-mass balance modelling, aiming at resolving the fine scale accumulation pattern across western DML.

ACKNOWLEDGEMENTS

REFERENCES

Arnold, N. and G. Rees. 2003. Self-similarity in glacier surface characteristics. *J. Glaciol.*, **49**(167), 547-554.

Arthern, R. J., D. P. Winebrenner and D. G. Vaughan (2006), Antarctic snow accumulation mapped using polarization of 4.3-cm wavelength microwave emission. *J. Geophys. Res.*, **111**, D06107, doi:10.1029/2004JD005667.

Bernhard, L. and R. Weibel. 1999. Modelling snowmelt using a digital terrain model and GIS-based techniques. *In* R. Dikau and H. Sauer, *eds. GIS for earth surface systems. Analysis and modelling of the natural environment.* Gebrüder Borntraeger, Berlin.

Budd, W. F. and D. B. Carter. 1971. An analysis of the relation between the surface and bedrock profiles of ice caps. *J. Glaciol.,* **10**(59), 197-209.

Burrough, P.A. 1986. Principles of Geographical Information Systems for Land Resources Assessment. New York, Oxford University Press.

Chainey, S., N. Stuart. 1998. Stochastic simulation: an alternative interpolation technique for digital geographic information. In Carver, S., *ed., Innovations in GIS 5*. London, UK, Taylor & Francis Ltd.

Eisen, O., W. Rack, U. Nixdorf and F. Wilhelms. 2005. Characteristics of accumulation around the EPICA deep-drilling site in Dronning Maud Land, Antarctica. *Ann. Glaciol.*, **41**, 41-46.

Frezzotti, M., M. Pourchet, O. Flora, S. Gandolfi, M. Gay, S. Urbini, C. Vincent, S. Becagli, R. Gragnani, M. Proposito, M. Severi, R. Traversi, R. Udisti and M. Fily. 2004. New estimations of precipitation and surface sublimation in East Antarctica from snow accumulation measurements. *Climate Dyn.*, **23**, 803–813.

Frezzotti, M., M. Pourchet, O. Flora, S. Gandolfi, M. Gay, S. Urbini, C. Vincent, S. Becagli, R. Gragnani, M. Proposito, M. Severi, R. Traversi, R. Udisti and M. Fily. 2005. Spatial and temporal variability of snow accumulation in East Antarctica from traverse data. *J. Glaciol.*, **51**(172), 113-124.

Giovinetto, M.B. and C.R. Bentley. 1985. Surface balance in ice drainage systems of Antarctica. *Antarct. J. U. S.*, **20**, 6 –13.

Giovinetto, M.B., N.M. Waters and C.R. Bentley. 1990. Dependence of Antarctic surface mass balance on Temperature, Elevation, and Distance to open ocean. J. Geophys. Res., **95**(D4), 3517-3531.

Giovinetto, M.B. and H.J. Zwally. 2000. Spatial distribution of net surface accumulation on the Antarctic ice sheet. *Ann. Glaciol.*, **31**, 171-178.

Goodwin, I.D. 1991. Snow-accumulation variability from seasonal surface observations and firn-core stratigraphy, eastern Wilkes Land, Antarctica. *J. Glaciol.*, **37**(127), 383-387.

Graf, W., H. Oerter, O. Reinwarth, W. Stichler, F. Wilhelms, H. Miller and R. Mulvaney. 2002. Stable-isotope records from Dronning Maud Land, Antarctica. *Ann. Glaciol.*, **35**, 195-201.

Hofstede, M., R.S.W. Van deWal, K.A. Kaspers, M.R. Van den Broeke, L. Karlöf, J.-G. Winther, E. Isaksson, G. Lappegard, R. Mulvaney, H. Oerter and F.Wilhelms. 2004. Firn accumulation records for the past 1000 years on the basis of dielectric profiling of six cores from Dronning Maud Land, Antarctica. J. Glaciol., 50(169), 279-291.

Holmlund, P. and J.-O. Näslund. 1994. The glacially sculptured landscape in Dronning Maud Land, Antartica, formed by wet-based mountain glaciation and not by the present ice sheet. *Boreas* **23**, 139-148.

Huybrechts, P., D. Steinhage, F. Wilhelms and J. Bamber. 2000. Balance velocities and measured properties of the Antarctic ice sheet from a new compilation of gridded data for modelling. *Ann. Glaciol.*, **30**, 52-60.

Isaksson, E. and W. Karlén. 1994. Spatial and temporal patterns in snow accumulation and oxygen isotopes, Western Dronning Maud Land, Antarctica. *J. Glaciol.*, **40**(135), 399-409.

Isaksson, E., W. Karlén, N. Gundestrup, P. Mayewski, S. Whitlow and M. Twickler. 1996. A century of accumulation and temperature changes in Dronning Maud Land, Antarctica. *J. Geophys. Res.*, **101**(D3), 7085-7094.

Isaksson, E., M.R. Van den Broeke, J.-G. Winther, L. Karlöf, J.F. Pinglot and N. Gundestrup. 1999. Accumulation and proxy-temperature variability in Dronning Maud Land, Antarctica, determined from shallow firn cores. *Ann. Glaciol.*, **29**, 17-22.

Journel, A.G. 1986. Geostatistics: Models and tools for the earth sciences. *J. of the International Association for Mathematical Geology*, **18**(1), 119-140.

Karlöf, L., J.-G. Winther, E. Isaksson, J. Kohler, J.F. Pinglot, F. Wilhelms, M. Hansson, P. Holmlund, M. Nyman, R. Pettersson and M. Stenberg. 2000. A 1500 years record of accumulation at Amundsenisen western Dronning Maud Land, Antarctica, derived from electrical and radioactive measurements on a 120 m ice core. *J. Geophys. Res.*, **105**(D10), 12,471-12,483.

Kaczmarska, M., Karlöf, L., Isaksson, E., Winther, J-G., Godtliebsen, F., Hofstede, C.M., Van den Broeke, M.R., Van de Wal, R.S.W. & Gundestrup, N. 2004. Accumulation variability derived from an ice core from coastal Dronning Maud Land, Antarctica. *Ann. Glaciol.*, **39**, 339-345.

King, J.C., P.S. Anderson, D.G. Vaughan, G.W. Mann, S.D. Mobbs and S.B. Vosper. 2004. Wind-borne redistribution of snow across an Antarctic ice rise. *J. Geophys. Res.*, **109**(D11104), doi:10.1029/2003JD004361.

Liu, H., K. Jezek, B. Li and Z. Zhao. 2001. Radarsat Antarctic Mapping Project digital elevation model version 2. Digital media, National Snow and Ice Data Center, Boulder, CO, USA.

Lunde, T. 1961. On the snow accumulation in Dronning Maud Land. *Nor. Polarinst. Skr.* 123.

Melvold, K., J.O. Hagen, J.F. Pinglot and N. Gundestrup. 1998. Large spatial variation in accumulation rate in Jutulstraumen ice stream, Dronning Maud Land, Antarctica. *Ann. Glaciol.*, **27**, 231-238.

Melvold, K. 1999. Impact of recent climate on glacier mass balance: studies on Kongsvegen, Svalbard, and Jutulstraumen, Antarctica. (D.Sc. thesis, University of Oslo.) (Department of Geography Report 13.)

Morgan, V.I. 1985. An oxygen isotope – climate record from the Law Dome, Antarctica. *Clim. Change*, **7**, 415-426.

Morgan, V.I., I.D. Goodwin, D.M. Etheridge and C.W. Wookey. 1991. Evidence from Antarctic ice cores for recent increases in snow accumulation. *Nature*, **354**(6348), 58-60.

Mosley-Thompson, E., P. D. Kruss, L. G. Thompson, M. Pourchet and P. Grootes. 1985. Snow stratigraphic record at South Pole: potential for paleoclimatic reconstruction. *Ann. Glaciol.*, **7**, 2633.

Mosley-Thompson, E. 1992. Paleoenvironmental conditions in Antarctica since A.D. 15000: Ice core evidence. *In* R.S. Bradley and P.D. Jones, *eds. Climate since A.D. 1500*. Routledge, New York.

Mulvaney, R. and E. Wolff. 1993. Evidence for winter spring denitrification of the stratosphere in the nitrate record of Antartic firn cores. *J. Geophys. Res.*, **98**(D3), 5213-5220.

Noone, D., J. Turner and R. Mulvaney. 1999. Atmospheric signals and characteristics of accumulation in Dronning Maud Land, Antarctica. *J. Geophys. Res.*, **104**(D16), 19,191-19,211.

Oerter, H., W. Graf, F. Wilhelms, A. Minikin and H. Miller. 1999. Accumulation studies on Amundsenisen, Dronning Maud Land, Antartica, by means of tritium, dielectric profiling and stable-isotope measurements: first results from the 1995-97 field seasons. *Ann. Glaciol.*, **29**, 1-9.

Oerter, H., F. Wilhelms, F. Jung-Rothenhäusler, F. Göktas, H. Miller, W. Graf and S. Sommer. 2000. Accumulation rates in Dronning Maud Land, Antartica, as revealed by dielectric-profiling measurements of shallow firn cores. *Ann. Glaciol.*, **30**, 27-34.

Petit, J.R., J. Jouzel, M. Pourchet and L. Merlivat. 1982. A detailed study of snow accumulation and stable isotope content in Dome C (Antarctica), *J. Geophys. Res.*, **87**(C6), 4301-4308.

Picciotto, E., G. Grozaz and W. De Breuck. 1971. Accumulation on the South Pole-Queen Maud Land Traverse, 1964-1968. Antarctic Snow and Ice Studies II, *Antarc. Res. Ser.*, **16**, 257-315.

Reijmer, C. and M.R. Van den Broeke. 2003. Temporal and spatial variability of the surface mass balance in Dronning Maud Land, Antarctica, as derived from automatic weather stations. *J. Glaciol.*, **49**(167), 512-520.

Richardson, C. and P. Holmlund. 1999. Spatial variability at shallow snow-layer depths in central Dronning Maud Land, East Antarctica. *Ann. Glaciol.*, **29**, 10-16.

Richardson-Näslund, C., E. Aarholt, S.-E. Hamram, P. Holmlund and E. Isaksson. 1997. Spatial distribution of snow in western Dronning Maud Land, East Antarctica, mapped by a ground-based snow radar. *J. Geophys. Res.*, **102**(B9), 20,343-20,353.

Richardson-Näslund, C. 2004. Spatial characteristics of snow accumulation in Dronning Maud Land, Antarctica. *Global and Planetary Change*, **42**, 31-43.

Rotschky, G., O. Eisen, F. Wilhelms, U. Nixdorf and H. Oerter. 2004. Spatial distribution of surface mass balance on Amundsenisen plateau, Antarctica, derived from ice-penetrating radar studies. *Ann. Glaciol.*, 39, 265-270.

Rotschky, G., W. Rack. W. Dierking, H. Oerter. 2006. Retrieving snowpack properties and accumulation estimates from a combination of SAR and scatterometer measurements. *IEEE Trans. Geosci. Remote Sens.*, **44**(4), 943-956.

Schlosser, E., H. Oerter and W. Graf. 1999. Surface mass balance investigations on Ekströmisen, Antarctica,1980-1996. Ber. Polarforsch. / *Rep. Pol. Res.*, 313.

Sommer, S., C. Appenzeller, C., R. Röthlisberger, M.A. Hutterli, B. Stauffer, D. Wagenbach, H. Oerter, F. Wilhelms, H. Miller and R. Mulvaney. 2000. Glacio-chemical study spanning the past 2 kyr on three ice cores from Dronning Maud Land, Antarctica. 1. Annually resolved accumulation rates. *J. Geophys. Res.*, **105**(D24), 29,411-29,421.

Spikes, V.B., G.S. Hamilton, S.A. Arcone, S. Kaspari and P. Mayewski. 2004. Variability in accumulation rates from GPR profiling on the West Antarctic plateau. *Ann. Glaciol.*, **39**, 238-244.

Stenberg, M., E. Isaksson, M. Hansson, W. Karlén, P.A. Mayewski, M.S. Twickler, S.I. Whitlow, and N. Gundestrup. 1998. Spatial variability of snow chemistry in western Dronning Maud Land, Antartica. *Ann. Glaciol.*, **27**, 378-384.

Stenberg, M., M. Hansson, P. Holmlund and L. Karlöf. 1999. Variability in snow layering and snow chemistry in the vicinity of two drill sites in western Dronning Maud Land, Antarctica. *Ann. Glaciol.*, **29**, 33-37.

Van den Broeke, M.R., J.-G. Winther, E. Isaksson, J.F. Pinglot, L. Karlöf, T. Eiken and L. Conrads. 1999. Climate variables along a traverse line in Dronning Maud Land, East Antarctica. *J. Glaciol.*, **45**(150), 295-302.

Van den Broeke, M. R., W. J. van de Berg and E. van Meijgaard. 2006. Snowfall in coastal West Antarctica much greater than previously assumed, *Geophys. Res. Lett.,* **33**, L02505, doi:10.1029/2005GL025239.

Van Lipzig, N.P.M., J. Turner, S.R. Colwell and M.R. Van den Broeke. 2004. The near-surface wind field over the Antarctic continent. *Int. J. Climatol.*, **24**, 1973-1982.

Vaughan, D.G., J. L. Bamber, M. B. Giovinetto, J. Russell and A. P.R. Cooper. 1999. Reassessment of net surface mass balance in Antarctica. *J. Climate*, **12**(4), 933-946.

Wackernagel, H. 1998. Multivariate geostatistics: an introduction with applications. Berlin, Springer.

Wolff, E. and E. Suttie. 1994. Antarctic snow record of southern-hemisphere lead pollution. *Geophys. Res. Let.*, **21**(9), 781 – 784.

APPENDIX

List of firn/ice core (C) and snow pit (P) measurements sampled over the area of interest (also available from the PANGEA Web site http://doi.pangaea.de/10.1594/PANGAEA.407654). Records included (i) in the interpolation are marked with a "y" in the first row.

	Site name		Institution / Campaign	Year drilled	Lat	Lon	Period	A $kg\ m^{-2}a^{-1}$	Dating Method	Reference
y	SPQML_01	P	SPQMLT 03	1967/68	79°08'S	36°43'E	1955-1968	35	total β	Picciotto and others (1971)
y	SPQML_02	P	SPQMLT 03	1967/68	78°51'S	33°14'E	1955-1968	37	total β	Picciotto and others (1971)
y	SPQML_03	P	SPQMLT 03	1967/68	78°43'S	29°43'E	1955-1968	35	total β	Picciotto and others (1971)
y	SPQML_04	P	SPQMLT 03	1967/68	78°35'S	27°05'E	1955-1968	36	total β	Picciotto and others (1971)
y	SPQML_05	P	SPQMLT 03	1967/68	78°19'S	23°22'E	1955-1968	25	total β	Picciotto and others (1971)
y	SPQML_06	P	SPQMLT 03	1967/68	78°01'S	20°05'E	1955-1968	19	total β	Picciotto and others (1971)
y	SPQML_07	P	SPQMLT 03	1967/68	77°39'S	17°10'E	1955-1968	29	total β	Picciotto and others (1971)
y	SPQML_08	P	SPQMLT 03	1967/68	77°16'S	14°25'E	1955-1968	45	total β	Picciotto and others (1971)
y	SPQML_09	P	SPQMLT 03	1967/68	76°50'S	11°53'E	1955-1968	52	total β	Picciotto and others (1971)
y	SPQML_10	P	SPQMLT 03	1967/68	76°22'S	09°32'E	1955-1968	45	total β	Picciotto and others (1971)
	SPQML_11	P	SPQMLT 03	1967/68	75°56'S	07°13'E	1955-1968	51	total β	Picciotto and others (1971)
y	SPQML_12	P	SPQMLT 03	1967/68	76°17'S	05°48'E	1955-1968	47	total β	Picciotto and others (1971)
y	SPQML_13	P	SPQMLT 03	1967/68	76°38'S	04°16'E	1955-1968	51	total β	Picciotto and others (1971)
y	SPQML_14	P	SPQMLT 03	1967/68	77°10'S	01°46'E	1955-1968	43	total β	Picciotto and others (1971)
y	SPQML_15	P	SPQMLT 03	1967/68	77°30'S	00°05'E	1955-1968	42	total β	Picciotto and others (1971)
y	SPQML_16	P	SPQMLT 03	1967/68	77°53'S	01°55'W	1955-1968	56	total β	Picciotto and others (1971)
y	SPQML_17	P	SPQMLT 03	1967/68	78°16'S	04°01'W	1955-1968	52	total β	Picciotto and others (1971)
y	SPQML_18	P	SPQMLT 03	1967/68	78°42'S	06°52'W	1955-1968	45	total β	Picciotto and others (1971)
y	B04	C	AWI	1981/82	70°37'S	8°22'W	1892-1981	353	$\delta^{18}O$, 3H	Schlosser and others (1999)
	FBKM002	C	AWI	1986/87	70°36'S	8°22'W	1972-1986	335	$\delta^{18}O$, ECM, 3H	this paper
y	FBKM40	C	AWI	1986/87	70°57'S	08°31'W	1971-1986	294	$\delta^{18}O$, ECM, 3H	Oerter and others (1999)
y	B12	C	AWI	1986/87	71°14'S	08°32'W	1961-1986	228	$\delta^{18}O$, ECM, 3H	Oerter and others (1999)
	FBKM70-W	C	AWI	1986/87	71°15'S	08°39'W	1979-1986	295	$\delta^{18}O$, ECM, 3H	this paper
y	FBKM90	C	AWI	1986/87	71°24'S	08°21'W	1969-1986	266	$\delta^{18}O$, ECM, 3H	Oerter and others (1999)
	SSKM125	P	AWI	1986/87	71°41'S	08°30'W	1982-1986	205	$\delta^{18}O$, ECM, 3H	Oerter and others (1999)
y	FBKM143	C	AWI	1986/87	71°50'S	08°37'W	1972-1986	229	$\delta^{18}O$, ECM, 3H	Oerter and others (1999)
y	FBKM160	C	AWI	1986/87	71°59'S	08°44'W	1969-1986	277	$\delta^{18}O$, ECM, 3H	Oerter and others (1999)
y	FBKM180	C	AWI	1986/87	72°10'S	08°50'W	1973-1986	364	$\delta^{18}O$, ECM, 3H	Oerter and others (1999)
y	B10, B11	C	AWI	1986/87	72°30'S	09°06'W	1970-1986	53	$\delta^{18}O$, ECM, 3H	Oerter and others (1999)
y	FBKM270	C	AWI	1986/87	72°56'S	09°41'W	1970-1986	46	$\delta^{18}O$, ECM, 3H	Oerter and others (1999)
y	BAS_CLA	C	BAS	1986/87	77°34'S	25°22'W	1964-1986	56	total β	Wolff and Suttie (1994)
y	BAS_H1	C	BAS	1987/88	77°02'S	22°32'W	1964-1987	155	nss, volc. horiz.	Mulvaney and Wolff (1993)
y	SW89_A	C	SWEDARP	1988/89	72°39'S	16°39'W	1976-1988	364	$\delta^{18}O$	Isaksson and Karlén (1994)
y	SW89_C	C	SWEDARP	1988/89	72°46'S	14°35'W	1976-1988	415	$\delta^{18}O$	Isaksson and Karlén (1994)
y	SW89_D	C	SWEDARP	1988/89	73°27'S	12°33'W	1976-1988	330	$\delta^{18}O$	Isaksson and Karlén (1994)
	SW89_E	C	SWEDARP	1988/89	73°36'S	12°26'W	1976-1988	311	$\delta^{18}O$	Isaksson and Karlén (1994)
y	SW89_F	C	SWEDARP	1988/89	73°49'S	12°13'W	1976-1988	217	$\delta^{18}O$	Isaksson and Karlén (1994)
y	SW89_G	C	SWEDARP	1988/89	74°01'S	12°01'W	1976-1988	276	$\delta^{18}O$	Isaksson and Karlén (1994)
y	SW89_H	C	SWEDARP	1988/89	74°21'S	11°43'W	1976-1988	329	$\delta^{18}O$	Isaksson and Karlén (1994)
y	SW89_J	C	SWEDARP	1988/89	75°05'S	09°32'W	1955-1988	104	total β	Isaksson and Karlén (1994)
y	SW92_E	C	SWEDARP	1991/92	73°36'S	12°26'W	1932-1991	324	$\delta^{18}O$, ECM	Isaksson and others (1996)
y	SW_EPCIA	C	SWEDARP	1991/92	75°00'S	02°00'E	1865-1991	77	CD (sodium, nitrate), volc. horiz.	Isaksson and others (1996)
y	SW92_1	C	SWEDARP	1991/92	74°10'S	00°22'E	1965-1993	116	total β	This paper
y	SW92_2	C	SWEDARP	1991/92	76°19'S	06°05'W	1955-1993	71	total β	This paper
y	Jut_A	C	NARE	1992/93	72°17'S	01°42'W	1976-1993	491	$\delta^{18}O$	Melvold (1999)
y	Jut_B	C	NARE	1992/93	72°08'S	01°46'W	1976-1993	487	$\delta^{18}O$	Melvold (1999)
y	Jut_C	C	NARE	1992/93	72°16'S	01°16'W	1976-1993	456	$\delta^{18}O$	Melvold (1999)
y	Jut_D	C	NARE	1992/93	72°31'S	01°46'W	1976-1993	491	$\delta^{18}O$	Melvold (1999)
y	Jut_E	C	NARE	1992/93	72°59'S	01°08'W	1965-1993	50	total β	Melvold (1998)
y	Jut_F	C	NARE	1992/93	73°06'S	00°28'W	1965-1993	120	total β	Melvold (1998)
y	Jut_H	C	NARE	1992/93	70°30'S	02°28'W	1976-1993	451	$\delta^{18}O$, total β	Melvold (1999)
y	Jut_I	C	NARE	1992/93	71°31'S	01°11'E	1965-1993	60	total β	Melvold (1998)
y	Jut_J	C	NARE	1992/93	72°13'S	00°43'W	1976-1993	320	$\delta^{18}O$, total β	Melvold (1999)
y	Jut_K	C	NARE	1992/93	70°45'S	00°00'E	1976-1993	253	$\delta^{18}O$, total β	Melvold (1999)
y	Jut_L	C	NARE	1992/93	70°56'S	00°13'E	1976-1993	244	$\delta^{18}O$, total β	Melvold (1999)
y	Jut_M	C	NARE	1992/93	70°25'S	00°00'W	1984-1993	371	$\delta^{18}O$, total β	Melvold (1999)
	SW93_1	P	SWEDARP	1993/94	73°28'S	12°34'W	1991-1993	280	CD (8 ions, $\delta^{18}O$)	Stenberg and others (1998)
y	SW93_2	P	SWEDARP	1993/94	74°58'S	11°48'W	1988-1993	120	CD (8 ions, $\delta^{18}O$)	Stenberg and others (1998)
y	SW93_3	P	SWEDARP	1993/94	78°02'S	10°59'W	1986-1993	90	CD (8 ions, $\delta^{18}O$)	Stenberg and others (1998)
y	SW93_4	P	SWEDARP	1993/94	75°33'S	09°46'W	1984-1993	70	CD (8 ions, $\delta^{18}O$)	Stenberg and others (1998)
y	SW93_5	P	SWEDARP	1993/94	75°29'S	09°05'W	1982-1993	60	CD (8 ions, $\delta^{18}O$)	Stenberg and others (1998)
y	SW93_7	P	SWEDARP	1993/94	75°30'S	04°35'W	1982-1993	60	CD (8 ions, $\delta^{18}O$)	Stenberg and others (1998)
y	SW93_9	P	SWEDARP	1993/94	75°30'S	02°41'E	1980-1993	50	CD (8 ions, $\delta^{18}O$)	Stenberg and others (1998)

	SW93_10	P	SWEDARP	1993/94	73°57'S	12°05'W	1991-1993	150	CD (8 ions, δ^{18}O)	Stenberg and others (1998)
	SW93_11	P	SWEDARP	1993/94	74°16'S	11°46'W	1991-1993	150	CD (8 ions, δ^{18}O)	Stenberg and others (1998)
	SW93_12	P	SWEDARP	1993/94	73°39'S	09°43'W	1990-1993	130	CD (8 ions, δ^{18}O)	Stenberg and others (1998)
	SW93_13	P	SWEDARP	1993/94	72°01'S	08°45'W	1992-1993	390	CD (8 ions, δ^{18}O)	Stenberg and others (1998)
y	FB96K02	C	AWI	1995/96	73°22'S	09°42'W	1964-1995	140	Artificial tritium (SS), ECM, DEP (volc. horiz.)	Oerter and others (1999)
y	FB96DML01	C	AWI	1995/96	74°52'S	02°33'W	1895-1995	41	ECM, DEP, nss, 3H	Oerter and others (1999)
y	FB96DML02	C	AWI	1995/96	74°58'S	03°55'E	1919-1995	59	ECM, DEP, nss, 3H	Oerter and others (1999)
y	FBWatz95-2	C	AWI	1995/96	70°56'S	07°24'W	1964-1995	173	δ^{18}O, 3H	This paper
y	S_{20}	C	NARE	1996/97	70°15'S	04°49'E	1965-1996	265	δ^{18}O, ECM	Isaksson and others (1999)
y	S_{15}	C	NARE	1996/97	71°12'S	04°36'E	1965-1996	244	δ^{18}O, ECM	Isaksson and others (1999)
y	A	C	NARE	1996/97	71°54'S	03°05'E	1965-1996	135	total β, ECM	Isaksson and others (1999)
y	B	C	NARE	1996/97	72°08'S	03°11'E	1965-1996	171	total β, ECM	Isaksson and others (1999)
y	C	C	NARE	1996/97	72°16'S	02°53'E	1965-1996	123	total β, ECM	Isaksson and others (1999)
y	D	C	NARE	1996/97	72°31'S	03°00'E	1965-1996	116	total β, ECM	Isaksson and others (1999)
y	E	C	NARE	1996/97	72°41'S	03°40'E	1965-1996	59	total β, ECM	Isaksson and others (1999)
y	F	C	NARE	1996/97	72°52'S	04°21'E	1965-1996	24	total β, ECM	Isaksson and others (1999)
y	G	C	NARE	1996/97	73°03'S	05°03'E	1965-1996	30	total β, ECM	Isaksson and others (1999)
y	H	C	NARE	1996/97	73°24'S	06°28'E	1965-1996	46	total β, ECM	Isaksson and others (1999)
y	I	C	NARE	1996/97	73°44'S	07°56'E	1965-1996	53	total β, ECM	Isaksson and others (1999)
y	J	C	NARE	1996/97	74°03'S	09°30'E	1965-1996	52	total β, ECM	Isaksson and others (1999)
y	K	C	NARE	1996/97	74°22'S	11°06'E	1965-1996	44	total β, ECM	Isaksson and others (1999)
y	L	C	NARE	1996/97	74°39'S	12°47'E	1965-1996	41	total β, ECM	Isaksson and others (1999)
y	M	C	NARE	1996/97	75°00'S	15°00'E	1965-1996	45	total β	Isaksson and others (1999)
	FB97DML01	C	AWI	1996/97	74°52'S	02°33'W	1964-1996	46	ECM, DEP, nss	Oerter and others (1999)
	FB97DML03	C	AWI	1996/97	74°30'S	01°58'E	1941-1996	91	ECM, DEP, nss	Oerter and others (1999)
y	FB97DML04	C	AWI	1996/97	74°24'S	07°13'E	1905-1996	53	ECM, DEP, nss	Oerter and others (1999)
	FB97DML05	C	AWI	1996/97	75°00'S	00°01'E	1930-1996	71	ECM, DEP, nss	Oerter and others (1999)
y	FB97DML06	C	AWI	1996/97	75°00'S	08°01'E	1899-1996	50	ECM, DEP, nss	Oerter and others (1999)
	FB97DML07	C	AWI	1996/97	75°35'S	03°26'W	1908-1996	57	ECM, DEP, nss	Oerter and others (1999)
y	FB97DML08	C	AWI	1996/97	75°45'S	03°17'E	1919-1996	60	ECM, DEP, nss	Oerter and others (1999)
y	FB97DML09	C	AWI	1996/97	75°56'S	07°13'E	1897-1996	45	ECM, DEP, nss	Oerter and others (1999)
y	FB97DML10	C	AWI	1996/97	75°13'S	11°21'E	1900-1996	47	ECM, DEP, nss	Oerter and others (1999)
	FB96K01	C	AWI	1996/97	74°13'S	09°45'W	1962-1995	125	ECM, DEP, nss	Oerter and others (2000)
y	FB9801	C	AWI	1997/98	70°43'S	08°26'W	1948-1997	317	ECM, CFA, nss	Oerter and others (2000)
y	FB9802	C	AWI	1997/98	74°13'S	09°45'W	1881-1997	129	ECM, CFA, nss	Oerter and others (2000)
y	FB9809	C	AWI	1997/98	74°30'S	01°58'E	1801-1997	89	ECM, CFA, nss	Oerter and others (2000)
y	B32	C	AWI	1997/98	75°00'S	00°01'E	1801-1997	62	ECM, CFA, nss	Oerter and others (2000)
y	FB9806	C	AWI	1997/98	75°00'S	00°02'E	1816-1997	62	ECM, CFA, nss	Oerter and others (2000)
y	FB9807	C	AWI	1997/98	75°00'S	00°02'E	1816-1997	67	CFA, nss	Oerter and others (2000)
y	B31	C	AWI	1997/98	75°35'S	03°26'W	1801-1997	59	ECM, CFA, nss	Oerter and others (2000)
y	SS9801	P	AWI	1997/98	74°51'S	08°30'W	1989-1997	76	ECM, CFA, nss	Oerter and others (2000)
y	FB9817	C	AWI	1997/98	75°00'S	06°30'W	1816-1998	62	CFA, nss	Oerter and others (2000)
y	FB9816	C	AWI	1997/98	75°00'S	04°30'W	1800-1997	47	CFA, nss	Oerter and others (2000)
y	FB9815	C	AWI	1997/98	74°57'S	01°30'W	1801-1997	53	CFA, nss	Oerter and others (2000)
y	FB9814	C	AWI	1997/98	75°05'S	02°30'E	1801-1997	64	ECM, CFA, nss	Oerter and others (2000)
y	FB9813	C	AWI	1997/98	75°10'S	05°00'E	1816-1997	48	CFA, nss	Oerter and others (2000)
y	B33	C	AWI	1997/98	75°10'S	06°30'E	1801-1997	47	ECM, CFA, nss	Oerter and others (2000)
y	FB9804	C	AWI	1997/98	75°15'S	06°00'W	1801-1997	50	ECM, CFA, nss	Oerter and others (2000)
y	FB9805	C	AWI	1997/98	75°10'S	01°00'W	1810-1997	44	ECM, CFA, nss	Oerter and others (2000)
y	FB9808	C	AWI	1997/98	74°45'S	01°00'E	1801-1997	68	ECM, CFA, nss	Oerter and others (2000)
y	FB9810	C	AWI	1997/98	74°40'S	04°00'E	1801-1997	86	CFA, nss	Oerter and others (2000)
y	FB9811	C	AWI	1997/98	75°05'S	06°30'E	1801-1997	58	CFA, nss	Oerter and others (2000)
y	FB9812	C	AWI	1997/98	75°15'S	06°30'E	1816-1997	38	CFA, nss	Oerter and others (2000)
y	FB9818	C	AWI	1998/99	74°27'S	09°27'W	1958-1999	169	DEP, δ^{18}O	This paper
y	FB9903	C	AWI	1999/00	74°50'S	00°01'E	1931-1999	80	DEP, δ^{18}O	This paper
y	FB9904	C	AWI	1999/00	75°03'S	00°42'E	1935-1999	68	DEP, δ^{18}O	This paper
y	CV	C	SWEDARP	1997/98	76°00'S	08°03'W	1810-1997	62	volc. horiz. (DEP/ECM), total β	Karlöf and others (2000)
y	M1	C	BAS	1997/98	77°01'S	10°26'W	1816-1997	70	total β	This paper
y	M4	C	BAS	1997/98	77°03'S	10°20'W	1955-1997	63	total β	This paper
y	M5	C	BAS	1997/98	77°00'S	10°33'W	1955-1997	69	total β	This paper
y	M6	C	BAS	1997/98	77°01'S	06°40'W	1955-1997	68	total β	This paper
y	BAS-Depot	C	BAS	1997/98	77°02'S	10°30'W	965-1998	71	DEP (volc. horiz.)	Hofstede and others (2004)
	M150	C	NARE	2000/01	75°00'S	15°00'E	965-1998	43	DEP (volc. horiz.)	Hofstede and others (2004)
y	FB0501	C	AWI	2004/05	74°09'S	09°41'W	1975-2004	183	δ^{18}O, DEP	This paper

ECM Electrical conductivity method DEP Dielectric profiling CD Chemical data SS Sea salt
NSS Non-sea-salt sulphate (volcanic eruptions) δ^{18}O Oxygen-isotope stratigraphy CFA Continuous Flow Analysis